metals

MDPI

Review

The Prospects of Zinc as a Structural Material for Biodegradable Implants—A Review Paper

Galit Katarivas Levy [1,*], Jeremy Goldman [2] and Eli Aghion [1]

[1] Department of Materials Engineering, Ben-Gurion University of the Negev, P.O. Box 652, 8410501 Beer-Sheva, Israel; egyon@bgu.ac.il

[2] Biomedical Engineering Department, Michigan Technological University, Houghton, MI 49931, USA; jgoldman@mtu.edu

* Correspondence: levyga@post.bgu.ac.il; Tel.: +972-50-6944074

Received: 31 August 2017; Accepted: 22 September 2017; Published: 1 October 2017

Abstract: In the last decade, iron and magnesium, both pure and alloyed, have been extensively studied as potential biodegradable metals for medical applications. However, broad experience with these material systems has uncovered critical limitations in terms of their suitability for clinical applications. Recently, zinc and zinc-based alloys have been proposed as new additions to the list of degradable metals and as promising alternatives to magnesium and iron. The main byproduct of zinc metal corrosion, Zn^{2+}, is highly regulated within physiological systems and plays a critical role in numerous fundamental cellular processes. Zn^{2+} released from an implant may suppress harmful smooth muscle cells and restenosis in arteries, while stimulating beneficial osteogenesis in bone. An important limitation of pure zinc as a potential biodegradable structural support, however, lies in its low strength (σ_{UTS} ~30 MPa) and plasticity ($\varepsilon < 0.25\%$) that are insufficient for most medical device applications. Developing high strength and ductility zinc with sufficient hardness, while retaining its biocompatibility, is one of the main goals of metallurgical engineering. This paper will review and compare the biocompatibility, corrosion behavior and mechanical properties of pure zinc, as well as currently researched zinc alloys.

Keywords: zinc; zinc alloys; biodegradable; biocompatible; corrosion degradation; mechanical properties

1. Introduction

Over the last 4 decades, innovations in biomaterials and medical technology have attracted remarkable attention for their potential to improve human life, by replacing and repairing soft and hard tissues, such as bone, cartilage, blood vessels, or even entire organs [1,2]. During this time, metals have become widely used as orthopedic implants, cardiovascular interventional devices, and tissue engineering scaffolds, due to their high strength and toughness compared with polymers and ceramic materials [3,4]. Traditional metallic biomaterials with high corrosion resistance, such as titanium alloys, stainless steels, cobalt–chromium alloys and tantalum are generally used as permanent implants in patients [3–5]. In most applications, however, the function of the implant is temporary and no longer needed after full recovery of the treated site. Furthermore, the permanent presence of the implant can lead to chronic deleterious effects. For instance, metal ions can be released from implanted devices due to defects in the surface oxide film, eventually resulting in implant fracture. In other cases, a chronic inflammatory response against the implant may undermine the therapeutic function of the device. In such circumstances, a second operation may be necessary to extract the implant, resulting in additional injury and expense [1,3,6,7].

Biodegradable metals represent an alternative approach to the traditional paradigm of corrosion resistant metals [1,8]. Biodegradable metals are expected to corrode gradually and harmlessly in vivo, maintain mechanical integrity during the critical tissue healing phase, and then dissolve completely

upon fulfilling their mission [8]. In the last decade, iron and magnesium, both pure and alloyed, have been extensively studied as potential biodegradable metals for medical applications [8–15]. However, broad experience with these material systems has uncovered critical limitations in terms of their suitability for clinical applications [5,16–22]. For instance, the corrosion rates for Fe and Fe-based alloys are generally substantially below clinical needs, producing similar problems as found with permanent implants [8,16,23,24]. Their corrosion products do not appear to be excreted or metabolized at a satisfactory rate, but rather accumulate and repel neighboring cells and biological matrices, rather than allowing cells to integrate around and within the original footprint of the degrading implant [25]. On the other hand, pure and alloyed Mg exhibits insufficient mechanical strength as well as excessive corrosion rates, accompanied by hydrogen gas evolution, pH increases, and premature loss of mechanical integrity [7,26–29].

Recently, zinc and zinc-based alloys were proposed as new additions to the list of degradable metals and as promising alternatives to magnesium and iron [30–34]. The following are advantageous characteristics of zinc and its alloys for use in medical applications:

- Similar to magnesium and iron, zinc is an essential trace element in the human body. It is a component of more than 300 enzymes and an even greater number of other proteins, highlighting its indispensable role in human health. Optimal nucleic acid and protein metabolism, as well as cell growth, division, and function, require sufficient availability of zinc [30,35]. From this perspective, zinc ions released from the implant during the degradation phase could integrate into the normal metabolic activity of the host without producing systemic toxic side effects [36].
- Zinc exhibits high chemical activity, with an electrode potential (−0.762 V) falling between that of magnesium (−2.372 V) and iron (−0.444 V) [36–38]. Pure zinc metal, therefore, exhibits moderate degradation rates (faster than the slowly degrading Fe and its alloys, but slower than the rapidly degrading Mg and its alloys) due to passive layers of moderate stability, formed by corrosion products [19,39–41].
- Zinc and zinc-based alloys are easier to cast and process due to their low melting points, low chemical reactivity and good machinability [37,42,43]. For instance, unlike Mg based alloys, the melting of zinc alloys can more conveniently be performed in air [37].

An important limitation of pure zinc as a potential biodegradable structural support, lies in its low strength (σ_{UTS} ~30 MPa) and plasticity ($\varepsilon < 0.25\%$) characteristics that are insufficient for most medical applications [42,44,45]. Developing zinc with high strength and sufficient hardness is one of the main goals of metallurgical engineering, to broaden its utility as a biomedical implant. One of the most powerful tools to improve a metal's mechanical performance is the addition of alloying elements to the pure metal matrix [36,44]. Researchers have developed Zn-based alloys with new and more attractive features, modifying their chemical composition and microstructure, in order to improve mechanical properties, by principally using solid solution and second-phase strengthening [45]. Furthermore, improvements in the mechanical properties of pure zinc can be produced by the thermomechanical refinement of grain size, by extrusion, rolling, etc. [9]. This paper will review and compare the biocompatibility, corrosion behavior and mechanical properties of pure zinc as well as currently researched zinc alloys. The various types of zinc alloys, in terms of compositions and phase constituents, are summarized in Table 1.

Table 1. Common biomedical zinc alloys.

Family	Representive Alloys and Alloying Elements (wt %)	Main Phases	References
Zn–Mg	Zn–0.15Mg	α-Zn, Mg_2Zn_{11}	[9]
	Zn–0.5Mg	α-Zn, Mg_2Zn_{11}	[9]
	Zn–1Mg, ZnMg1	α-Zn, Mg_2Zn_{11}	[9,22,42,46,47]
	Zn–1.2Mg	α-Zn, Mg_2Zn_{11}	[3]
	Zn–1.5Mg, ZnMg1.5	α-Zn, Mg_2Zn_{11}	[36,42]
	Zn–3Mg, ZnMg3	α-Zn, Mg_2Zn_{11}	[9,42,48]
	Zn–1.5Mg–0.1Ca	α-Zn, Mg_2Zn_{11}, $CaZn_{13}$	[36]
	Zn–1Mg–0.5Ca	α-Zn, Mg_2Zn_{11}, $CaZn_{13}$	[47]
	Zn–1Mg–1Ca	α-Zn, Mg_2Zn_{11}, $CaZn_{13}$	[44]
	Zn–1Mg–0.1Sr	Zn, $MgZn_2$, $SrZn_{13}$	[49]
	Zn–1Mg–0.5Sr	Zn, $MgZn_2$, $SrZn_{13}$	[49]
	Zn–1.5Mg–0.1Sr	α-Zn, Mg_2Zn_{11}, $SrZn_{13}$	[36]
	Zn–1Mg–1Sr	α-Zn, Mg_2Zn_{11}, $SrZn_{13}$	[44]
	Zn–1Mg–0.1Mn	Zn, $MgZn_2$	[50]
	Zn–1.5Mg–0.1Mn	Zn, $MgZn_2$	[50]
Zn–Ca	Zn–1Ca	α-Zn, $CaZn_{13}$	[22]
	Zn–1Ca–1Sr	α-Zn, $CaZn_{13}$, $SrZn_{13}$	[44]
Zn–Sr	Zn–1Sr	α-Zn, $SrZn_{13}$	[22]
Zn–Al	Zn–0.5Al	Zn, Al	[9,51]
	Zn–1Al	Zn, Al	[9,52]
	Zn–3Al	Zn, Al	[52]
	Zn–5Al	Zn, Al	[52]
	ZnAl4Cu1	Zn, Al	[42]
	ZA0.1Mg	α-Zn, $Mg_2(Zn,Al)_{11}$	[51]
	ZA0.3Mg	α-Zn, $Mg_2(Zn,Al)_{11}$	[51]
	ZA0.5Mg/Zn-0.5Al-0.5Mg	α-Zn, $Mg_2(Zn,Al)_{11}$	[51,53]
	Zn–0.5Al–0.5Mg–0.1Bi	Zn, $Mg_2(Zn,Al)_{11}$, Mg_3Bi_2	[53]
	Zn–0.5Al–0.5Mg–0.3Bi	Zn, $Mg_2(Zn,Al)_{11}$, Mg_3Bi_2	[53]
	Zn–0.5Al–0.5Mg–0.5Bi	Zn, $Mg_2(Zn,Al)_{11}$, Mg_3Bi_2	[53]
	3.5–.5Al, 0.75–1.25Cu, 0.03–0.08Mg	Zn, Al	[3]
	3.5–4.3Al, 2.5–3.2Cu, 0.03–0.06Mg	Zn, Al	[3]
	5.6–6Al, 1.2–1.6Cu	Zn, Al	[3]
Zn–Cu	Zn–1Cu	η-Zn, ε-$CuZn_5$	[54]
	Zn–2Cu	η-Zn, ε-$CuZn_5$	[54]
	Zn–3Cu	η-Zn, ε-$CuZn_5$	[54,55]
	Zn–4Cu	η-Zn, ε-$CuZn_5$	[37,54]
	Zn–3Cu–0.1Mg	Zn, $CuZn_5$, Mg_2Zn_{11}	[55]
	Zn–3Cu–0.5Mg	Zn, $CuZn_5$, Mg_2Zn_{11}	[55]
	Zn–3Cu–1Mg	Zn, $CuZn_5$, Mg_2Zn_{11}	[55]
Zn–Li	Zn–2Li	Zn, α-$LiZn_4$	[25]
	Zn–4Li	Zn, α-$LiZn_4$	[25]
	Zn–6Li	Zn, α-$LiZn_4$	[25]
	Zn–Li	Zn, α-$LiZn_4$	[56]
Zn–Ag	Zn–2.5Ag	η-Zn, ε-$AgZn_3$	[45]
	Zn–5Ag	η-Zn, ε-$AgZn_3$	[45]
	Zn–7Ag	η-Zn, ε-$AgZn_3$	[45]

2. Zinc in the Human Body

The essential role of zinc in the human body was discovered in 1961 when Iranian farmers subsisting on a zinc deficiency diet (unrefined flat bread, potatoes, and milk) were found to suffer from a group of syndromes, consisting of anemia, hypogonadism, and dwarfism. Since this discovery, interest in the biochemical and clinical aspects of zinc has increased markedly [57]. Presently, it is well known that zinc is one of the most abundant nutritionally essential elements in the human body [44]. Zinc is present in all organs, tissues, fluids and body secretions, with 86% of its mass residing in skeletal muscle and bone, 6% in the skin, 5% in the liver, 1.5% in the brain and the remaining distributed amongst the other tissues [35,58]. At the cellular level, 30–40% is located in the nucleus,

50% in the cytoplasm, organelles and specialized vesicles (for digestive enzymes or hormone storage) and the remaining portion in the cell membrane [35,44]. The human zinc requirement is estimated at 15 mg/day [8,10,11,37] and due to its high importance, the body has developed sophisticated mechanisms to remove zinc from dietary constituents and transport it to desired locations. The human body is able to absorb zinc from the environment, regulate its concentration in body fluids, transport it safely to all tissues of the body and to the sites where its presence is required, and safely excrete excess amounts from the body through the kidneys [35].

As a vital element, zinc plays an important role in numerous physiological systems, including immune, sexual, neurosensory (cognition and vision), and cell development and growth [19,30]. Zinc participates in numerous fundamental biological functions, such as nucleic acid metabolism, signal transduction, apoptosis regulation, and gene expression [22]. Zinc is a critical component of enzymes involved in protein synthesis and energy production. More than 1200 proteins are predicted to contain, bind, or transport Zn^{2+}, for example, zinc-finger proteins [44]. At the cellular level, zinc maintains the structural integrity of biomembranes and is essential for cell proliferation, differentiation and signaling [19,59]. Zinc plays an important role in bone formation, mineralization, and preservation of bone mass and can be found in the bone extracellular matrix, where it is co-deposited with calcium hydroxyapatite [19,22,60]. Indeed, a zinc decrease in bone matrix correlates with aging and skeletal disease [22,61].

Table 2 summarizes the systemic symptoms resulting from zinc deficiency or excess. Zinc deficiency contributes to retarded growth, impaired parturition (dystocia), neuropathy, decreased food intake, diarrhea, dermatitis, hair loss, bleeding tendencies, hypotension, and hypothermia [44]. Zinc deficiency is generally due to insufficient dietary intake. However, it may also be a consequence of malabsorption and chronic illnesses, such as diabetes, malignancy, liver disease, and sickle cell disease [35,57]. On the other hand, excessive amounts of Zn^{2+} in the body may be detrimental to vital organs, such as the kidney, liver, spleen, brain, and heart [19]. In addition, a prolonged overdose of zinc results in copper deficiency, provokes hypocupremia, anemia, leucopenia, and neutropenia, and impairs the Cu–Zn–superoxide dismutase antioxidant enzyme [30,62].

Table 2. The systemic symptoms resulting from zinc deficiency and excess [35,63,64].

Organ or System	Zinc Deficiency	Zinc Excess
Brain	Decreased nerve conduction, neuropsychiatric and neurosensory disorders, mental lethargy	Lethargy, focal neuronal deficits.
Respiratory tract	-	Respiratory disorder after inhalation of zinc smoke, metal fume fever.
Immune system	Impaired immune system function, increased susceptibility to pathogens	Altered lymphocyte function.
Thymus	Thymic atrophy	-
Skin	Skin lesions, decreased wound healing, acrodermatitis	-
Gastrointestinal tract	-	Nausea/vomiting, epigastric pain, diarrhea.
Reproductive system	Infertility, retarded genital development, hypogonadism	-
Prostate	-	Elevated risk of prostate cancer.

3. Corrosion Behavior of Zinc in the Physiological Environment

The degradation model, proposed by Zheng et al. [8], for biodegradable metals in a neutral physiological environment, generally occurs via cathodic and anodic reactions. Metallic corrosion produces hydroxides, oxides, and hydrogen gas by-products [65]. In the specific case of zinc, as presented in Figure 1, the reactions include a number of intermediate species, according to the following:

$$\text{Anodic} \quad \text{reaction}: \ 2Zn \rightarrow 2Zn^{2+} + \overline{4}e^{-} \tag{1}$$

$$\text{Cathodic reaction}: \ O_2 + 2H_2O + \overline{4}e^- \rightarrow 4OH^- \quad (2)$$

$$Zn(OH)_2 \text{ formation}: \ 2Zn^{2+} + 4OH^- \rightarrow 2Zn(OH)_2 \quad (3)$$

$$\text{ZnO formation}: \ Zn(OH)_2 \rightarrow ZnO + H_2O \quad (4)$$

When exposed to body fluid, zinc is oxidized into metal cations following the anodic reaction in Equation (1). The generated electrons are consumed by a cathodic reaction, corresponding to the dissolved oxygen reduction in Equation (2). $Zn(OH)_2$ and ZnO corrosion products are likely to form on the metal surface, without gas evolution, according to Equations (3) and (4). Hence, gas release is not expected as a result of zinc corrosion, in contrast to the highly problematic hydrogen gas that is released as a byproduct of magnesium corrosion [8,30,36,59].

It should be noted that the physiological environment is highly aggressive, particularly due to the high concentration of chloride ions. These ions destabilize the equilibrium between dissolution and formation of the corrosion product layer, given that chloride ions are able to convert the surface into soluble chloride salts as follows:

$$6Zn(OH)_2 + Zn^{2+} + 2Cl^- \rightarrow 6Zn(OH)_2 \cdot ZnCl_2 \quad (5)$$

$$4ZnO + 4H_2O + Zn^{2+} + 2Cl^- \rightarrow 4Zn(OH)_2 \cdot ZnCl_2 \quad (6)$$

The dissolution of the $Zn(OH)_2$ and ZnO surface film components promotes further dissolution of the exposed metal. Cycles of cathodic and anodic reactions expose the fresh metal substrate to the physiological solution, form corrosion products, and convert the product into soluble salts. With progressive exposure, an irregular particle may be separated from the zinc matrix and enter the surrounding medium [8,36].

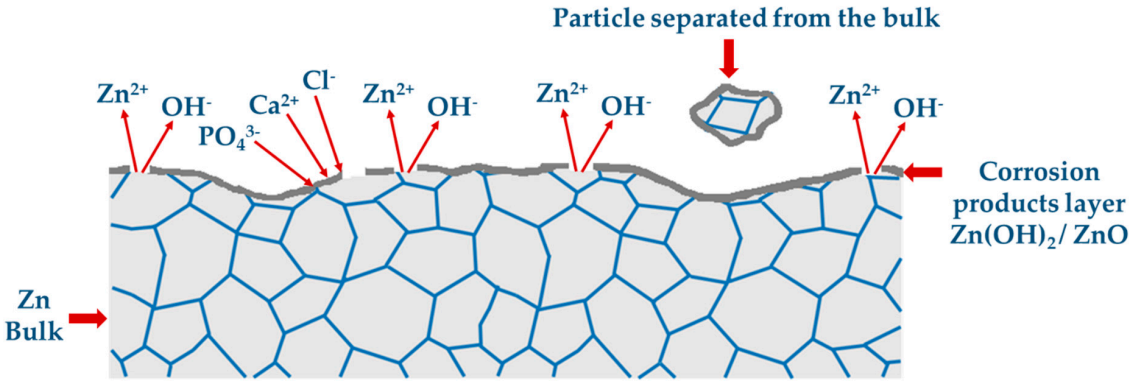

Figure 1. Model of the zinc degradation process in physiological fluids.

According to Bowen et al. [59], thin layers of zinc oxide were the only product observed during early stages (1.5 and 3 months) on the surface of zinc wires (99.99% purity) implanted into rat aorta. However, as corrosion progressed to 4.5 and 6 months, the corrosion layer thickened and contained three different phases/layers: calcium phosphate, zinc oxide, and zinc carbonate. The calcium phosphate layer appeared on the exterior surface without forming a true bulk product. Hence, the calcium phosphate layer was not thought to play a significant role in zinc biocorrosion. The compact corrosion layer included the two other phases, zinc oxide, and zinc carbonate, with ZnO appearing in formations isolated from one another by the zinc carbonate phase. This complex corrosion layer suggests that corrosion products of zinc in body fluid might be similar to those reported for magnesium. These ceramic degradation products can accumulate as a function of the local tissue's physiological mass transfer rate and therefore may impact tissue healing and remodeling [30,59].

Another important factor that needs to be considered in the corrosion of zinc is the pH value of the solution. According to Pourbaix diagram, shown in Figure 2, zinc is present as hydrated $Zn^{2+}_{(aq)}$, over the entire physiological range of pH values and biological standard reduction potentials (~820 mV to ~−670 mV). The purple arrow in Figure 2 indicates the range of biologically-important standard potentials determined at pH 7.4 [66]. As reported by Thomas et al. [67] in their investigation of zinc corrosion as a function of pH, in the pH range 7 to 10, the lowered cathodic reaction rates reduce overall zinc corrosion rates, and the surface oxides thermodynamically predicted to form in this pH range do not form an effective corrosion protection barrier. Hence, zinc metals in physiological environments with a pH of 7.4 will be dissolved over time, as is required for biodegradable medical implants.

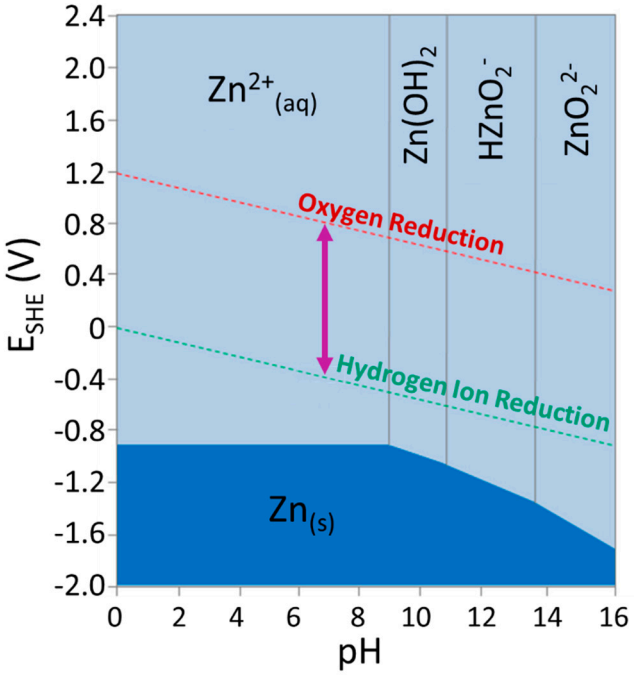

Figure 2. Pourbaix diagram of zinc. The purple arrow shows the range of biological standard reduction potentials at pH 7.4: from ~820 mV to ~−670 mV [66].

4. Biocompatibility and Biological Performances of Zinc and Evaluated Zinc Alloys

4.1. Pure Zinc

After implantation, Zn^{2+} will be released from the zinc implant to the surrounding extracellular space and eventually into the bloodstream. Thus, the cellular responses to high extracellular Zn^{2+} will impact the healing process and biocompatibility with zinc-bearing implants [16]. Furthermore, the response of the host's immune system will determine whether the implant becomes biointegrated and continues to function as designed, or encapsulated in a dense fibrous tissue that may compromise the intended function of the implant. The inflammatory cells are sensitive to the implant's corrosion behavior and cellular accessibility of the surface product, with more porous and actively corroding interfaces eliciting more benign inflammatory responses, relative to surfaces that are more resistant to biocorrosion [20,68]. The inflammatory response can therefore potentially be regulated by controlling implant degradation behavior and rates through alloying and processing.

4.1.1. In Vitro Examination

Törne et al. [32] investigated the initial degradation of zinc exposed to simulated (phosphate buffered saline (PBS), Ringer's saline solution) and physiological body fluids (human plasma, whole blood). They found a decrease in the corrosion rate over time when immersed in body fluids and

an increase when placed in simulated body fluids. The passivation film that formed in physiological body fluids was uniform and was composed of inorganic corrosion products and organic materials (biomolecules). In contrast, the simulated body fluids promoted localized corrosion with thick porous products, primarily composed of zinc phosphates and carbonates.

The cellular response of human bone marrow mesenchymal stem cells (hMSC) and human vascular cells (HCECs, HASMC, HAEC) to Zn^{2+} was recently investigated [16,26,69,70]. According to Zhu et al. [70], Zn biomaterial can support hMSC adhesion and proliferation and zinc ions can lead to enhanced regulation of genes, cell survival/growth and differentiation, extracellular matrix (ECM) mineralization, and osteogenesis. The stimulation of osteogenesis by ionic zinc has been supported by numerous studies [71–79]. In the case of human vascular cells, Zn^{2+} at low concentrations can enhance cell viability, proliferation, adhesion, spreading, migration, and F-actin and vinculin expression, while decreasing cell adhesion strength. In contrast, high concentrations of Zn^{2+} elicited opposite effects. Gene expression profiles revealed that the most affected functional genes were related to angiogenesis, inflammation, cell adhesion, vessel tone, and platelet aggregation [26]. Since the Zn^{2+} concentration is intrinsically related to the implant degradation rate, a slow corrosion rate with controlled release of Zn^{2+} is desirable to maintain a low concentration profile of Zn^{2+} in the local tissues, in order to benefit cellular functions [16]. A high concentration of Zn^{2+} may overwhelm metal divalent ion-dependent intracellular signaling pathways, stimulate oxidative stress pathways, inducing apoptosis or necrosis, and generally contribute to negative side effects in cell populations adjacent to the implant.

4.1.2. In Vivo Examination

Bowen et al. studied the in vivo performance of zinc wires (99.99%) over 6 months when implanted into the abdominal aorta of adult rats [59,80]. They found uniform corrosion with linearly increasing corrosion rates over the residence time. The corrosion rate after 1.5 months was below the 0.02 mm/year degradable stent benchmark and increased to 0.05 mm/year (~0.4 and ~0.97 mg/day, respectively) after 6 months, both of which are far below the daily allowance of zinc (15 mg/day) [59]. In addition, a histological examination indicated excellent biocompatibility with the arterial tissue as well as tissue regeneration within the original footprint of the degrading implant. Intriguingly, observations of low cellular density and a distinct lack of smooth muscle cells adjacent to the implant interface indicates that the Zn^{2+} ions released from a zinc implant may suppress restenosis pathways [80]. Yang et al. [81] investigated the degradation of pure zinc stents over one year in a rabbit abdominal aorta model. They reported an excellent biocompatibility, without severe inflammation, platelet aggregation, thrombosis formation or obvious intimal hyperplasia. The degradation rates were matched to the artery healing process. Moreover, the pure zinc stent retained its mechanical integrity for 6 months and degraded to 41.75 $\pm$ 29.72% of its original volume after 12 months of implantation.

4.2. Zinc Alloys

The biocompatibility of absorbable biomaterial components must be considered, given that all elements of the metal alloy will eventually pass through the human body [10]. Table 3 summarizes the pathophysiology and toxicology of zinc and the alloying elements used in current zinc alloys. Table 4 lists the corrosion performance of different zinc alloys, including their in vitro and in vivo corrosion rates. In Table 4, the Zn–0.5Al–0.5Mg–0.5Bi alloy exhibits the highest corrosion rate (0.28 mm/year), which for standard implants is still far below the daily allowance of zinc (15 mg/day). The tabulated data supports the notion that zinc release during the stent degradation process should be considered safe to human systems, although toxicity at the local level will need to be examined on a case-by-case basis.

In the ideal design of degradable biomaterials, elements with potential toxicological effects should be avoided, and their use should be minimized if they cannot be excluded [10]. Since Mg, Ca, Cu, Mn and Sr are essential for humans, these elements should be the first choices as alloying elements for biomedical zinc alloys. Li et al. studied the in vitro and in vivo performance of Zn-1X binary alloys

with the nutrient alloying elements, Mg, Ca and Sr [22]. The in vitro results for human morphologies on the Zn–1X alloy surfaces, and generated pseudopods and extrace umbilical vein endothelial cells ECV304 and Human osteosarcoma MG63 demonstrated healthy cell llular matrix secretions, compared to an unhealthy morphology for cells cultured on pure Zn. When experimental Zn–1X pins were implanted into mouse femurs, new bone formation in the absence of inflammation was observed around the implantation site, in particular for the Zn–1Sr alloy. The corrosion rates of the Zn–1X pins were 0.17, 0.19 and 0.22 mm/year for Zn–1Mg, Zn–1Ca and Zn–1Sr pins, respectively, which is far below the daily allowance of zinc [22]. Even when adding higher amounts of Mg (3 wt %) to pure zinc, to a concentration of 0.75 mg/mL (Zn: 0.49 ppm and Mg: 10.75 ppm), the Zn–3Mg alloy extract exhibited acceptable cytotoxic effects on human osteoblasts. Results of the three main parameters of cell–material interaction, which includes cell health, cell functionality, and inflammatory responses, demonstrated acceptable cellular toxicity [19]. The addition of Mn to the Zn–Mg system increased the susceptibility for galvanic micro-cell corrosion due to the higher electrode potential of Mn [50]. The Zn–*x*Cu system exhibited a slightly increased corrosion rate with increasing Cu concentrations, compared to pure Zn, but the increase was not significantly different among the Zn–*x*Cu alloys. In vitro testing demonstrated the cytocompatibilty of Zn–*x*Cu alloys with human endothelial cells as well as an antibacterial property when the Cu concentration was above 2 wt % [54]. The addition of 0.1–1% Mg to the Zn–3Cu system increased the corrosion rate, as Mg was added [55].

The second choice of alloying element should be those that have been found to improve the properties of magnesium alloys, including Li and Al. However, given the potential toxicity of Li and Al, the addition of these two elements should be limited to low weight percent alloys. Moreover, the degradation rate of zinc alloys containing these elements should match the tolerance or effective dose range of these elements in the human body. Zhao et al. [25,56] investigated the effect of Li as a zinc alloying element. They reported the overall quantities of lithium released from a zinc–lithium implant (with 0.7 wt % of Li) at two orders of magnitude below the daily bodily consumption allowances. The in vivo implantation of Zn–1Li demonstrated positive biocompatibility, with no significant differences in serum zinc observed before, and 1–3 months after, implantation. According to Bowen et al. [52], biodegradation of a Zn–Al stent, with a weight of ~50 mg and a 5 wt % Al content—assuming bioabsorption of the entire stent in 2 years and a stable corrosion rate—would result in a daily intake of ~0.003 mg of Al, substantially below the ~10 mg daily intake for an average person. In their in vivo studies [20,52], Zn–Al (1, 3 and 5% Al) strips were implanted in the wall of the abdominal aorta of adult Sprague–Dawley rats. The Zn–Al systems exhibited acceptable compatibility with surrounding arterial tissue, as the histopathological analysis failed to identify necrotic tissue in the samples examined, although indications of chronic and acute inflammation were both identified. Moreover, the pattern of corrosion was modified through Al additions, with intergranular corrosion observed in all Zn–Al alloys. Intergranular corrosion accelerates the oxidation of zinc to zinc oxide, whose volume expansion produces implant cracking and fragmentation. The addition of 0.1–0.5 wt % Mg to the Zn–Al system decreased the corrosion rate with increasing Mg content, after 720 h of immersion in simulated body fluid (SBF) solution. The cytotoxicity results demonstrated acceptable biocompatibility of the Zn–0.5Al–0.5Mg alloy, with superior antibacterial activity relative to the other alloys [51].

Presently, the pathophysiology and toxicology of Ag and Bi remain unclear. Silver has been used clinically for decades to treat burns and assist with wound healing, due to its antibacterial properties, and has diverse medical applications [45,82,83]. Bi is generally considered less toxic than other heavy metal elements, such as antimony, and purified bismuth metal has been used to prepare a number of pharmaceutical products [53,83]. In two studies, the addition of Ag (2.5–7%) to pure zinc matrix and the addition of Bi (0.1–0.5%) to ternary Zn–Al–Mg alloy slightly increased the degradation rate. This is likely due to the increased galvanic coupling between the Zn and $AgZn_3/Mg_3Bi_2$ secondary phases [45,53]. In vitro cytotoxicity tests indicated a more toxic effect on MC3T3-E1 cells for Zn–Al–Mg–Bi alloys, compared to the Zn–Al–Mg alloy [53].

Table 3. Summary of the pathophysiology and toxicology of zinc and select alloying elements [8,10,11,83] and their effect on zinc alloys.

Element	Blood Serum Level	Daily Allowance	Pathophysiology	Toxicology	Effect on Zinc Alloys
Essential Elements					
Mg	17.7–25.8 mg/L	700 mg	Activator of many enzymes; co-regulator of protein synthesis and muscle contraction; stabilizer of DNA and RNA	Excessive Mg leads to nausea	Mg: ↑mechanical properties & ↑corrosion rates [22]
Ca	36.8–39.8 mg/L	800 mg	More than 99% have structural functions in the skeleton; the solution Ca has signaling functions, including muscle contraction, blood clotting, cell function, etc.	Inhibit the intestinal absorption of other essential minerals	Ca: ↑mechanical properties & ↑corrosion rates [22]
Fe	5000–17,600 mg/L	10–20 mg	Component of several metalloproteins; crucial in vital biochemical activities, i.e., oxygen sensing and transport	Iron toxicity gives rise to lesions in the gastrointestinal tract, shock and liver damage	Fe: ↑corrosion rates by galvanic corrosion mechanism [15]
Essential Trace Elements					
Zn	0.8–1.14 mg/L	15 mg	Trace element; appears in all enzyme classes; most Zn appears in muscle	Neurotoxic and hinders bone development at higher concentrations	-
Cu	4.51–8.32 mg/L	1–3 mg	Cu plays a vital role in the immune system; has beneficial effects on endothelial cell proliferation and has been reported to enhance antibacterial properties [55]	Excessive Cu (>1 mg/day) can cause neurodegenerative diseases, including Alzheimer's, Menkes and Wilson's diseases [55]	↑Cu (1–4%): ↑mechanical properties & ↑corrosion rates [37,54]
Mn	<0.0008 mg/L	4 mg	Activator of enzymes; Mn deficiency is related to osteoporosis, diabetes mellitus, and atherosclerosis	Excessive Mn results in neurotoxicity	Mn improves the casting process. Mn ↑ susceptibility of galvanic micro-cell corrosion [50]
Other Elements					
Sr	0.17 mg [a]	2 mg	99% is located in bone; shows dose dependent metabolic effects on bone; low doses stimulate new bone formation	High doses induce skeletal abnormalities	Sr: ↑mechanical properties & ↑corrosion rates [22]
Li	0.002–0.004 mg/L	0.2–0.6 mg	Used in the treatment of manic depressive psychoses	Plasma concentrations of 2 mM are associated with reduced kidney function and neurotoxicity, 4 mM may be fatal	Li: ↑ultimate tensile strength, ↓ductility & ↓corrosion rate [56]
Al	0.0021–0.0048 mg/L	-	-	Primarily accumulates in the bone and nervous systems; implicated in the pathogenesis of Alzheimer's disease; can cause muscle fiber damage; decreases osteoblast viability	Al: ↑mechanical properties & ↑corrosion rates

[a] Sr concentration in total blood [8].

Table 4. In vitro and in vivo corrosion rates of different zinc alloys.

Alloy	In Vitro Corrosion Rate		In Vivo Corrosion Rate (mm/year)	References
	Electrochemical (μA/cm^2)	Immersion (mm/year)		
Zn	1.8–9.2 (Hank's) 0.05 (plasma) 0.04 (whole blood) 0.035 (PBS)	0.027–0.13 (Hank's)	0.02–0.05 (1.5–6 months)	[9,20,22,23,31,32,45,53,59]
Zn *	8.98	-	-	[9]
		Zn–Mg		
Zn–0.15Mg [c]	11.52 (Hank's)	0.17 (Hank's)	-	[9]
Zn–0.15Mg [*,c]	10.98 (Hank's)	-	-	[9]
Zn–0.5Mg [c]	11.73 (Hank's)	0.175 (Hank's)	-	[9]
Zn–0.5Mg [*,c]	11.01 (Hank's)	-	-	[9]
Zn–1Mg [f]/ZnMg1 [b]	9.9–11.9 (Hank's) 0.28–1.2 (SBF) 0.74 (PBS)	0.085–0.18 (Hank's) 0.06–0.28 (SBF) 0.027 (PBS)	0.17	[9,22,42,46,47]
Zn–1Mg *	11.32 (Hank's)	0.12 (SBF)	-	[9,46]
Zn–1.2Mg	7.7 (Hank's)	0.08 (Hank's)	-	[3]
Zn–1.2Mg *	12.4 (Hank's)	0.11 (Hank's)	-	[3]
Zn–1.5Mg [d]/ZnMg1.5 [b]	8.8 (SBF)	0.063 (Hank's) 0.05 (SBF)	-	[4,36]
Zn–3Mg/ZnMg3 [b]	9.01 (Hank's) 7.4 (SBF)	0.13 (Hank's) 0.06–0.21 (SBF)	-	[9,42,48]
Zn–3Mg *	8.6 (Hank's)	-	-	[9]
Zn–3Mg ***	-	0.13 (SBF)	-	[48]
Zn–1.5Mg–0.1Ca [d]	-	0.12 (Hank's)	-	[36]
Zn–1Mg–0.5Ca	4.3 (PBS)	0.37 (PBS)		[47]
Zn—1Mg–1Ca [e]	0.17 (Hank's)	0.09 (Hank's)	-	[44]
Zn—1Mg–0.1Sr	7.85 (Hank's)	-	-	[49]
Zn–1Mg–0.5Sr	7.83 (Hank's)	-	-	[49]
Zn–1.5Mg–0.1Sr [d]	-	0.1 (Hank's)	-	[36]
Zn–1Mg–1Sr [e]	0.175 (Hank's)	0.095 (Hank's)	-	[44]
Zn–1Mg–0.1Mn	17.21 (Hank's)	0.12 (Hank's)	-	[50]
Zn–1.5Mg–0.1Mn	9.34 (Hank's)	0.09 (Hank's)	-	[50]
		Zn–Ca		
Zn–1Ca [f]	10.75 (Hank's)	0.09 (Hank's)	0.19	[22]
Zn–1Ca–1Sr [e]	0.185 (Hank's)	0.11 (Hank's)	-	[44]
		Zn–Sr		
Zn–1Sr [f]	11.76 (Hank's)	0.095 (Hank's)	0.22	[22]
		Zn–Al		
Zn–0.5Al	11.08 (Hank's) 20 (SBF)	0.14 (Hank's) 15 (SBF)	-	[9,51]
Zn–0.5Al [*,c]	9.6 (Hank's)	-	-	[9]
Zn–1Al	11.11 (Hank's)	0.16 (Hank's)	-	[9]

Table 4. *Cont.*

Alloy	In Vitro Corrosion Rate		In Vivo Corrosion Rate (mm/year)	References
	Electrochemical (μA/cm^2)	Immersion (mm/year)		
Zn–1Al *	9.7 (Hank's)	-	-	[9]
ZnAl4Cu1 [b]	5.2 (SBF)	0.07 (SBF)	-	[42]
ZA0.1Mg	17 (SBF)	0.13 (SBF)	-	[51]
ZA0.3Mg	11.2 (SBF)	0.11 (SBF)	-	[51]
ZA0.5Mg/Zn–0.5Al–0.5Mg	9.5 (SBF)	0.11–0.15 (SBF)	-	[51,53]
Zn–0.5Al–0.5Mg–0.1Bi	12 (SBF)	0.17 (SBF)	-	[53]
Zn–0.5Al–0.5Mg–0.3Bi	16 (SBF)	0.2 (SBF)	-	[53]
Zn–0.5Al–0.5Mg–0.5Bi	23 (SBF)	0.28 (SBF)	-	[53]
ZA4–1	2.986 (Hank's)	-	-	[31]
ZA4–3	7.209 (Hank's)	-	-	[31]
ZA6–1	5.331 (Hank's)	-	-	[31]
Zn–Cu				
Zn–1Cu *,[a]	-	0.033 (c-SBF)	-	[54]
Zn–2Cu *,[a]	-	0.027 (c-SBF)	-	[54]
Zn–3Cu *,[a]	0.372 (Hank's)	0.012 (Hank's) 0.03 (c-SBF)	-	[54,55]
Zn–4Cu *,[a]	4.1 (Hank's)	0.009 (Hank's) 0.025 (c-SBF)	-	[37,54]
Zn–3Cu–0.1Mg *	1.18 (Hank's)	0.023 (Hank's)	-	[55]
Zn–3Cu–0.5Mg *	1.56 (Hank's)	0.03 (Hank's)	-	[55]
Zn–3Cu–1Mg *	12.4 (Hank's)	0.0432 (Hank's)	-	[55]
Zn–Ag				
Zn–2.5Ag	9.2 (Hank's)	0.079 (Hank's)	-	[45]
Zn–5Ag	9.7 (Hank's)	0.081 (Hank's)	-	[45]
Zn–7Ag	9.9 (Hank's)	0.084 (Hank's)	-	[45]
Zn–Li				
Zn–2Li	0.011 (SBF)	-	-	[25]
Zn–4Li	0.004 (SBF)	-	-	[25]
Zn–6Li	0.0038 (SBF)	-	-	[25]
Zn–1Li	-	-	0.02–0.05	[56]

SBF: simulated body fluid; PBS: phosphate buffered saline; * Hot extrusion; *** Homogenisation; [a] Data gathered from figure in literature [54] (Figure 7); [b] Data gathered from figure in literature [42] (Figure 5b); [c] Data gathered from figure in literature [9] (Figure 12); [d] Data gathered from figure in literature [36] (Figure 5); [e] Data gathered from figure in literature [44] (Figure 7); [f] Data gathered from figure in literature [22] (Figure 3b).

5. Mechanical Properties of Zinc Alloys

Implanted biomaterials, such as bone plates and stents, should be compatible with the mechanical properties of the substituted tissue [10]. Table 5 compares the mechanical properties of zinc and current zinc-based alloys to bone and arterial tissues. It is apparent that the mechanical properties of pure zinc are insufficient for bone and arterial medical device applications, in particular compared to cortical bone. The most effective way to address this issue is by adding alloying elements and/or through the refinement of grain size by thermomechanical processing [9].

Zinc alloys exhibit a wide range of ultimate tensile strengths and elongations, from 87 to 399 MPa and from 0.9% to ~170%, respectively. It can be seen from Table 5 that even minor alloying can significantly improve mechanical properties; for example, adding 0.15% Mg to pure zinc improves its ultimate tensile strength from 18 MPa to 250 MPa, and the elongation fraction from 0.32% to 22% [9,44]. Moreover, hot rolling and hot extrusion contribute to the strength and ductility of zinc alloys [3,9,44,46]. For example: the yield strength (YS), ultimate tensile strength (UTS) and elongation of as-cast Zn–1Mg–1Ca are 80 MPa, 130 MPa, and 1%, respectively. Meanwhile, the YS, UTS and elongation properties of Zn-based ternary alloy samples are improved to 138 MPa, 197 MPa, and 8.5% after hot rolling and 205 MPa, 250 MPa, and 5.2% after hot extrusion, respectively [44]. Therefore, it is feasible to satisfy strength requirements for zinc alloys through conventional metallurgical approaches.

Table 5. Mechanical properties of bone and arterial tissues, compared with current biomedical zinc alloys.

Tissue/Alloy	Mechanical Properties				References
	Yield Strength (YS) (MPa)	Ultimate Tensile Strength (UTS) (MPa)	Elongation (%)	Hardness (HV)	
Cortical bone	104.9–114.3	35–283	5–23	-	[10,11]
Cancellous bone	-	1.5–38	-	-	[10,11]
Arterial wall	-	0.5–1.72	-	-	[10,11]
Zn [c]	10	18	0.32	38	[44]
Zn [*,c]	35	60	3.5	-	[44]
Zn [**,c,d]	30–110	50–140	5.8–36	39	[44,52]
Zn–Mg					
Zn—0.15Mg *	114	250	22	52	[9]
Zn–0.5Mg *	159	297	13	65	[9]
Zn–1Mg/ZnMg1	180	340	6	75–86	[9,22,42,47]
Zn–1Mg [*,f]	175	250	12	-	[46]
Zn–1.2Mg	116	130	1.4	93	[3]
Zn–1.2Mg *	220	362	21	96	[3]
Zn-1.5Mg	112	150	1.3	155	[36]
Zn–3Mg/ZnMg3	-	104	2.3	201	[48]
Zn–3Mg *	291	399	1	117	[9]
Zn–3Mg ***	-	88	8.8	175	[48]
Zn–1.5Mg–0.1Ca	173	241	1.72	150	[36]
Zn–1Mg–0.5Ca	-	150	1.34	116	[47]
Zn–1Mg–1Ca [c]	80	130	1	90	[44]
Zn–1Mg–1Ca [*,c]	205	250	5.2	-	[44]
Zn–1Mg–1Ca [**,c]	138	197	8.5	105	[44]
Zn–1Mg–0.1Sr	109	133	1.4	94	[49]
Zn–1Mg–0.5Sr	129	144	1.1	109	[49]
Zn–1.5Mg–0.1Sr	130	209	2.0	145	[36]
Zn–1Mg–1Sr [c]	85	135	1.2	85	[44]
Zn–1Mg–1Sr [*,c]	200	250	7.3	-	[44]
Zn–1Mg–1Sr [**,c]	140	200	9.7	90	[44]
Zn–1Mg–0.1Mn	114	132	98	1.11	[50]
Zn–1.5Mg–0.1Mn	115	122	149	0.77	[50]

Table 5. *Cont.*

Tissue/Alloy	Mechanical Properties				References
	Yield Strength (YS) (MPa)	Ultimate Tensile Strength (UTS) (MPa)	Elongation (%)	Hardness (HV)	
Zn–Ca					
Zn–1Ca	119	165	2	73	[22]
Zn–1Ca–1Sr [c]	83	140	1.1	90	[44]
Zn–1Ca–1Sr *,[c]	210	260	6.8	-	[44]
Zn–1Ca–1Sr **,[c]	145	203	8.6	85	[44]
Zn–Sr					
Zn–1Sr	120	171	2	61	[22]
Zn–Al					
Zn–0.5Al *	119	203	33	59	[9]
Zn–1Al *	134	223	24	73	[9]
Zn–1Al **,[d]	190	220	24	-	[52]
Zn–3Al **,[d]	200	240	30	-	[52]
Zn–5Al **,[d]	240	300	16	-	[52]
ZnAl4Cu1	171	210	1	80	[42]
ZA0.1Mg	-	87	1.6	79	[51]
ZA0.3Mg	-	93	1.7	89	[51]
ZA0.5Mg/Zn–0.5Al–0.5Mg	-	92–102	1.73–2.1	94	[51,53]
Zn–0.5Al–0.5Mg–0.1Bi	-	102	2.4	102	[53]
Zn–0.5Al–0.5Mg–0.3Bi	-	108	2.7	109	[53]
Zn–0.5Al–0.5Mg–0.5Bi	-	98	1.97	99	[53]
ZA4–1	75	180	~112	50	[31]
ZA4–3	110	200	~130	55	[31]
ZA6–1	175	275	~170	65	[31]
Zn–Cu					
Zn–1Cu *	149	186	21	-	[54]
Zn–2Cu *	199	240	46	-	[54]
Zn–3Cu *	213	257	47	-	[54,55]
Zn–4Cu *	227–250	270	51	-	[37,54]
Zn–3Cu–0.1Mg *,[b]	340	355	5	-	[55]
Zn–3Cu–0.5Mg *,[b]	390	400	2	-	[55]
Zn–3Cu–1Mg *,[b]	427	441	0.9	-	[55]
Zn–Ag					
Zn–2.5Ag *,[a]	174	200	35	-	[45]
Zn–5Ag *,[a]	236	250	36	-	[45]
Zn–7Ag *,[a]	258	287	32	-	[45]
Zn–Li					
Zn–2Li **,[e]	240	360	14.2	98	[25]
Zn–4Li **,[e]	420	440	13.7	115	[25]
Zn–6Li **,[e]	470	560	2.2	136	[25]
Zn–1Li	238	274	17	97	[56]

* Hot extrusion; ** Hot rolling; *** Homogenisation; [a] Data gathered from figure in literature [45]; (Figure 8a); [b] Data gathered from figure in literature [55] (Figure 5b); [c] Data gathered from figure in literature [44] (Figures 3 and 4); [d] Data gathered from figure in literature [52] (Figure 7); [e] Data gathered from figure in literature [25] (Figure 7); [f] Data gathered from figure in literature [46] (Figure 8).

6. Concluding Remarks and Perspectives

The previous several years have seen rapid growth in the research and development of zinc-based medical devices, due to their biological and biodegradability properties that match the human body. Zn is one of the most abundant essential elements in the human body, playing essential roles in human health. Moreover, zinc overcomes the limitations inherent to iron and magnesium, both pure and alloyed. This includes more suitable corrosion rates as well as easier casting and processing. In this review, current research progress for zinc and zinc-based alloys has been presented and discussed.

In the case of pure zinc, in vivo studies have demonstrated a great potential for use as biodegradable stents. The degradation of pure zinc stents proceeded with excellent biocompatibility to local cells and tissue and was aligned with the time course of arterial healing. Although the pure zinc stent poorly retained its mechanical integrity during the healing phase, this can be overcome by using zinc alloys with superior strength.

Despite the advantages, the use of pure Zn as a biodegradable metal is limited due to its insufficient strength, plasticity and hardness for most medical applications. Adding alloying elements and refining grain sizes via thermomechanical processing are commonly applied to modify the mechanical properties of metallic materials. A number of zinc alloys have been developed with nontoxic and biocompatible alloying elements that have achieved suitable mechanical properties to serve as structure support for arteries or bone, with promising preliminary results in cell culture and small animal models. For instance, Zn–Mg and Zn–Al at alloying concentrations of less than one percent, have enhanced mechanical properties and achieved adequate strength and ductility, without using excessive quantities of potentially toxic alloying elements. The mechanical properties of these materials are generally enhanced considerably from the as-cast state, following extrusion to break up embrittling intermetallics and to refine the grain size. Because each biomedical device (e.g., stent, bone plate or screw, etc.) requires unique processing conditions that can dramatically change material properties, it is crucial to evaluate candidate materials through these processing steps.

Looking ahead, researchers are required to translate the wealth of biomedical research data into an understanding of how these materials will behave within test subjects. Hence, it will be important to clarify the molecular mechanisms that stimulate beneficial cellular remodeling activities in response to Zn^{2+} and the alloying element ions. Next generation zinc implants will need to have tailored corrosion rates in order to optimize favorable cellular responses and minimize toxicity and negative inflammatory reactions, specific to the host tissue.

Author Contributions: All the authors wrote the paper.

Conflicts of Interest: The authors declare no conflict of interest.

References

1. Katarivas Levy, G.; Aghion, E. Influence of heat treatment temperature on corrosion characteristics of biodegradable EW10X04 Mg alloy coated with Nd. *Adv. Eng. Mater.* **2016**, *18*, 269–276. [CrossRef]
2. Holzapfel, B.M.; Reichert, J.C.; Schantz, J.-T.; Gbureck, U.; Rackwitz, L.; Nöth, U.; Jakob, F.; Rudert, M.; Groll, J.; Hutmacher, D.W. How smart do biomaterials need to be? A translational science and clinical point of view. *Adv. Drug Deliv. Rev.* **2013**, *65*, 581–603. [CrossRef] [PubMed]
3. Shen, C.; Liu, X.; Fan, B.; Lan, P.; Zhou, F.; Li, X.; Wang, H.; Xiao, X.; Li, L.; Zhao, S. Mechanical properties, in vitro degradation behavior, hemocompatibility and cytotoxicity evaluation of Zn–1.2 Mg alloy for biodegradable implants. *RSC Adv.* **2016**, *6*, 86410–86419. [CrossRef]
4. Niinomi, M. Metallic biomaterials. *J. Artif. Organs* **2008**, *11*, 105–110. [CrossRef] [PubMed]
5. Katarivas Levy, G.; Ventura, Y.; Goldman, J.; Vago, R.; Aghion, E. Cytotoxic characteristics of biodegradable EW10X04 Mg alloy after nd coating and subsequent heat treatment. *Mater. Sci. Eng. C* **2016**, *62*, 752–761. [CrossRef] [PubMed]
6. Pospíšilová, I.; Soukupová, V.; Vojtěch, D. Influence of calcium on the structure and mechanical properties of biodegradable zinc alloys. In *Materials Science Forum*; Trans Tech Publication Ltd.: Stafa-Zurich, Switzerland, 2017; pp. 400–403.
7. Aghion, E.; Levy, G.; Ovadia, S. In Vivo behavior of biodegradable Mg–Nd–Y–Zr–Ca alloy. *J. Mater. Sci.* **2012**, *23*, 805–812. [CrossRef] [PubMed]
8. Zheng, Y.; Gu, X.; Witte, F. Biodegradable metals. *Mater. Sci. Eng. C* **2014**, *77*, 1–34. [CrossRef]
9. Mostaed, E.; Sikora-Jasinska, M.; Mostaed, A.; Loffredo, S.; Demir, A.; Previtali, B.; Mantovani, D.; Beanland, R.; Vedani, M. Novel zn-based alloys for biodegradable stent applications: Design, development and in vitro degradation. *J. Mech. Behav. Biomed. Mater.* **2016**, *60*, 581–602. [CrossRef] [PubMed]

10. Gu, X.-N.; Zheng, Y.-F. A review on magnesium alloys as biodegradable materials. *Front. Mater. Sci. China* **2010**, *4*, 111–115. [CrossRef]
11. Witte, F.; Hort, N.; Vogt, C.; Cohen, S.; Kainer, K.U.; Willumeit, R.; Feyerabend, F. Degradable biomaterials based on magnesium corrosion. *Curr. Opin. Solid State Mater. Sci.* **2008**, *12*, 63–72. [CrossRef]
12. Jablonská, E.; Vojtěch, D.; Fousová, M.; Kubásek, J.; Lipov, J.; Fojt, J.; Ruml, T. Influence of surface pre-treatment on the cytocompatibility of a novel biodegradable ZnMg alloy. *Mater. Sci. Eng. C* **2016**, *68*, 198–204. [CrossRef] [PubMed]
13. Demir, A.G.; Monguzzi, L.; Previtali, B. Selective laser melting of pure Zn with high density for biodegradable implant manufacturing. *Addit. Manuf.* **2017**, *15*, 20–28. [CrossRef]
14. Wang, C.; Yu, Z.; Cui, Y.; Zhang, Y.; Yu, S.; Qu, G.; Gong, H. Processing of a novel Zn alloy micro-tube for biodegradable vascular stent application. *J. Mater. Sci. Technol.* **2016**, *32*, 925–929. [CrossRef]
15. Luo, M.; Shen, W.; Wang, Y.; Allen, M. In Vitro Degradation of Biodegradable Metal Zn And Zn/Fe-Couples and Their Application as Conductors in Biodegradable Sensors. In Proceedings of the 2015 Transducers-2015 18th International Conference on Solid-State Sensors, Actuators and Microsystems (TRANSDUCERS), Anchorage, AK, USA, 21–25 June 2015; pp. 1370–1373.
16. Ma, J.; Zhao, N.; Zhu, D. Endothelial cellular responses to biodegradable metal zinc. *ACS Biomater. Sci. Eng.* **2015**, *1*, 1174–1182. [CrossRef] [PubMed]
17. Aghion, E.; Levy, G. The effect of Ca on the in vitro corrosion performance of biodegradable Mg-Nd-Y-Zr alloy. *J. Mater. Sci.* **2010**, *45*, 3096–3101. [CrossRef]
18. Levy, G.; Aghion, E. Effect of diffusion coating of Nd on the corrosion resistance of biodegradable Mg implants in simulated physiological electrolyte. *Acta Biomater.* **2013**, *9*, 8624–8630. [CrossRef] [PubMed]
19. Murni, N.; Dambatta, M.; Yeap, S.; Froemming, G.; Hermawan, H. Cytotoxicity evaluation of biodegradable Zn–3Mg alloy toward normal human osteoblast cells. *Mater. Sci. Eng. C* **2015**, *49*, 560–566. [CrossRef] [PubMed]
20. Guillory, R.J.; Bowen, P.K.; Hopkins, S.P.; Shearier, E.R.; Earley, E.J.; Gillette, A.A.; Aghion, E.; Bocks, M.; Drelich, J.W.; Goldman, J. Corrosion characteristics dictate the long-term inflammatory profile of degradable zinc arterial implants. *ACS Biomater. Sci. Eng.* **2016**, *2*, 2355–2364. [CrossRef]
21. Hakimi, O.; Ventura, Y.; Goldman, J.; Vago, R.; Aghion, E. Porous biodegradable EW62 medical implants resist tumor cell growth. *Mater. Sci. Eng. C* **2016**, *61*, 516–525. [CrossRef] [PubMed]
22. Li, H.; Xie, X.; Zheng, Y.; Cong, Y.; Zhou, F.; Qiu, K.; Wang, X.; Chen, S.; Huang, L.; Tian, L. Development of biodegradable Zn-1X binary alloys with nutrient alloying elements Mg, Ca and Sr. *Sci. Rep.* **2015**, *5*, 10719. [CrossRef] [PubMed]
23. Liu, X.; Sun, J.; Yang, Y.; Pu, Z.; Zheng, Y. In vitro investigation of ultra-pure Zn and its mini-tube as potential bioabsorbable stent material. *Mater. Lett.* **2015**, *161*, 53–56. [CrossRef]
24. Kubásek, J.; Vojtěch, D.; Jablonská, E.; Pospíšilová, I.; Lipov, J.; Ruml, T. Structure, mechanical characteristics and in vitro degradation, cytotoxicity, genotoxicity and mutagenicity of novel biodegradable Zn–Mg alloys. *Mater. Sci. Eng. C* **2016**, *58*, 24–35. [CrossRef] [PubMed]
25. Zhao, S.; McNamara, C.T.; Bowen, P.K.; Verhun, N.; Braykovich, J.P.; Goldman, J.; Drelich, J.W. Structural characteristics and in vitro biodegradation of a novel Zn-Li alloy prepared by induction melting and hot rolling. *Metall. Mater. Trans. A* **2017**, *3*, 1204–1215. [CrossRef]
26. Ma, J.; Zhao, N.; Zhu, D. Bioabsorbable zinc ion induced biphasic cellular responses in vascular smooth muscle cells. *Sci. Rep.* **2016**, *6*, 26661. [CrossRef] [PubMed]
27. Kubasek, J.; Vojtěch, D. Zn-based alloys as an alternative biodegradable materials. *Proc Met.* **2012**, *5*, 23–25.
28. Kubasek, J.; Pospisilova, I.; Vojtech, D.; Jablonska, E.; Ruml, T. Structural, mechanical and cytotoxicity characterization of as-cast biodegradable Zn–*x*Mg (x = 0.8%–8.3%) alloys. *Mater. Tehnol.* **2014**, *48*, 623–629.
29. Dunne, C.F.; Katarivas Levy, G.; Hakimi, O.; Aghion, E.; Twomey, B.; Stanton, K.T. Corrosion behaviour of biodegradable magnesium alloys with hydroxyapatite coatings. *Surf. Coat. Technol.* **2016**, *289*, 37–44. [CrossRef]
30. Seitz, J.M.; Durisin, M.; Goldman, J.; Drelich, J.W. Recent advances in biodegradable metals for medical sutures: A critical review. *Adv. Healthc. Mater.* **2015**, *4*, 1915–1936. [CrossRef] [PubMed]
31. Wang, C.; Yang, H.; Li, X.; Zheng, Y. In vitro evaluation of the feasibility of commercial Zn alloys as biodegradable metals. *J. Mater. Sci. Technol.* **2016**, *32*, 909–918. [CrossRef]

32. Törne, K.; Larsson, M.; Norlin, A.; Weissenrieder, J. Degradation of zinc in saline solutions, plasma, and whole blood. *J. Biomed. Mater. Res. Part B* **2016**, *104*, 1141–1151. [CrossRef] [PubMed]
33. Bolz, A.; Popp, T. Implantable, Bioresorbable Vessel Wall Support, in Particular Coronary Stent. U.S. Patent 6,287,332 B1, 11 September 2001.
34. Zhou, G.; Gongqi, Q.; Gong, H. Kind of Absorbable High Strength and Toughness Corrosion-Resistant Zinc Alloy Implant Material for Human Body. U.S. Patent 20170028107 A1, 2 February 2017.
35. Plum, L.M.; Rink, L.; Haase, H. The essential toxin: Impact of zinc on human health. *Int. J. Environ. Res. Public Health* **2010**, *7*, 1342–1365. [CrossRef] [PubMed]
36. Liu, X.; Sun, J.; Qiu, K.; Yang, Y.; Pu, Z.; Li, L.; Zheng, Y. Effects of alloying elements (Ca and Sr) on microstructure, mechanical property and in vitro corrosion behavior of biodegradable Zn–1.5Mg alloy. *J. Alloys Compd.* **2016**, *664*, 444–452. [CrossRef]
37. Niu, J.; Tang, Z.; Huang, H.; Pei, J.; Zhang, H.; Yuan, G.; Ding, W. Research on a Zn-Cu alloy as a biodegradable material for potential vascular stents application. *Mater. Sci. Eng. C* **2016**, *69*, 407–413. [CrossRef] [PubMed]
38. Huang, T.; Zheng, Y.; Han, Y. Accelerating degradation rate of pure iron by zinc ion implantation. *Regen. Biomater.* **2016**, *3*, 205–215. [CrossRef] [PubMed]
39. Vojtech, D.; Pospisilova, I.; Michalcova, A.; Maixner, J. Microstructure and mechanical properties of the micrograined hypoeutectic zn-mg alloy. *Int. J. Miner. Metall. Mater.* **2016**, *23*, 1167–1176.
40. Pospíšilová, I.; Vojtěch, D. Zinc alloys for biodegradable medical implants. In *Materials Science Forum*; Trans Tech Publlication: Stafa-Zurich, Switzerland, 2014; pp. 457–460.
41. Zhao, L.; Zhang, Z.; Song, Y.; Liu, S.; Qi, Y.; Wang, X.; Wang, Q.; Cui, C. Mechanical properties and in vitro biodegradation of newly developed porous Zn scaffolds for biomedical applications. *Mater. Des.* **2016**, *108*, 136–144. [CrossRef]
42. Vojtěch, D.; Kubásek, J.; Šerák, J.; Novák, P. Mechanical and corrosion properties of newly developed biodegradable Zn-based alloys for bone fixation. *Acta Biomater.* **2011**, *7*, 3515–3522. [CrossRef] [PubMed]
43. Guleryuz, L.; Ipek, R.; Arıtman, I.; Karaoglu, S. Microstructure and Mechanical Properties of Zn-Mg Alloys as Implant Materials Manufactured by Powder Metallurgy Method. In *AIP Conference Proceedings*; AIP Publishing: Melville, NY, USA, 2017.
44. Li, H.; Yang, H.; Zheng, Y.; Zhou, F.; Qiu, K.; Wang, X. Design and characterizations of novel biodegradable ternary Zn-based alloys with iia nutrient alloying elements mg, ca and sr. *Mater. Des.* **2015**, *83*, 95–102. [CrossRef]
45. Sikora-Jasinska, M.; Mostaed, E.; Mostaed, A.; Beanland, R.; Mantovani, D.; Vedani, M. Fabrication, mechanical properties and in vitro degradation behavior of newly developed ZnAg alloys for degradable implant applications. *Mater. Sci. Eng. C* **2017**, *77*, 1170–1181. [CrossRef] [PubMed]
46. Gong, H.; Wang, K.; Strich, R.; Zhou, J.G. In vitro biodegradation behavior, mechanical properties, and cytotoxicity of biodegradable Zn–Mg alloy. *J. Biomed. Mater. Res. Part B* **2015**, *103*, 1632–1640. [CrossRef] [PubMed]
47. Katarivas Levy, G.L.; Leon, A.; Kafri, A.; Ventura, Y.; Drelich, J.W.; Goldman, J.; Vago, R.; Aghion, E. Evaluation of biodegradable Zn–1%Mg and Zn–1%Mg–0.5%Ca alloys for biomedical applications. *J. Mater. Sci. Mater. Med.* **2017**. accepted. [CrossRef]
48. Dambatta, M.; Izman, S.; Kurniawan, D.; Farahany, S.; Yahaya, B.; Hermawan, H. Influence of thermal treatment on microstructure, mechanical and degradation properties of Zn–3Mg alloy as potential biodegradable implant material. *Mater. Des.* **2015**, *85*, 431–437. [CrossRef]
49. Liu, X.; Sun, J.; Yang, Y.; Zhou, F.; Pu, Z.; Li, L.; Zheng, Y. Microstructure, mechanical properties, in vitro degradation behavior and hemocompatibility of novel Zn–Mg–Sr alloys as biodegradable metals. *Mater. Lett.* **2016**, *162*, 242–245. [CrossRef]
50. Liu, X.; Sun, J.; Zhou, F.; Yang, Y.; Chang, R.; Qiu, K.; Pu, Z.; Li, L.; Zheng, Y. Micro-alloying with Mn in Zn–Mg alloy for future biodegradable metals application. *Mater. Des.* **2016**, *94*, 95–104. [CrossRef]
51. Bakhsheshi-Rad, H.; Hamzah, E.; Low, H.; Kasiri-Asgarani, M.; Farahany, S.; Akbari, E.; Cho, M. Fabrication of biodegradable Zn-Al-Mg alloy: Mechanical properties, corrosion behavior, cytotoxicity and antibacterial activities. *Mater. Sci. Eng. C* **2017**, *73*, 215–219. [CrossRef] [PubMed]

52. Bowen, P.; Seitz, J.; Guillory, R.; Braykovich, J.; Zhao, F.; Goldman, J.; Drelich, J. Evaluation of wrought Zn-Al alloys (1, 3, and 5 wt % al) through mechanical and in vivo corrosion testing for stent applications. *J. Biomed. Mater. Res. Part B* **2016**. [CrossRef]
53. Bakhsheshi-Rad, H.; Hamzah, E.; Low, H.; Cho, M.; Kasiri-Asgarani, M.; Farahany, S.; Mostafa, A.; Medraj, M. Thermal characteristics, mechanical properties, in vitro degradation and cytotoxicity of novel biodegradable Zn–Al–Mg and Zn–Al–Mg–xBi alloys. *Acta Metall. Sin. (Engl. Lett.)* **2017**, *30*, 201–211. [CrossRef]
54. Tang, Z.; Niu, J.; Huang, H.; Zhang, H.; Pei, J.; Ou, J.; Yuan, G. Potential biodegradable Zn-Cu binary alloys developed for cardiovascular implant applications. *J. Mech. Behav. Biomed. Mater.* **2017**, *72*, 182–191. [CrossRef] [PubMed]
55. Tang, Z.; Huang, H.; Niu, J.; Zhang, L.; Zhang, H.; Pei, J.; Tan, J.; Yuan, G. Design and characterizations of novel biodegradable Zn-Cu-Mg alloys for potential biodegradable implants. *Mater. Des.* **2017**, *117*, 84–94. [CrossRef]
56. Zhao, S.; Seitz, J.-M.; Eifler, R.; Maier, H.J.; Guillory, R.J.; Earley, E.J.; Drelich, A.; Goldman, J.; Drelich, J.W. Zn-Li alloy after extrusion and drawing: Structural, mechanical characterization, and biodegradation in abdominal aorta of rat. *Mater. Sci. Eng. C* **2017**, *76*, 301–312. [CrossRef] [PubMed]
57. Roohani, N.; Hurrell, R.; Kelishadi, R.; Schulin, R. Zinc and its importance for human health: An integrative review. *J. Res. Med. Sci.* **2013**, *18*, 144. [PubMed]
58. Jackson, M. Physiology of zinc: General aspects. In *Zinc in Human Biology*; Springer: Berlin, Germany, 1989; pp. 1–14.
59. Bowen, P.K.; Drelich, J.; Goldman, J. Zinc exhibits ideal physiological corrosion behavior for bioabsorbable stents. *Adv. Mater.* **2013**, *25*, 2577–2582. [CrossRef] [PubMed]
60. Moonga, B.S.; Dempster, D.W. Zinc is a potent inhibitor of osteoclastic bone resorption in vitro. *J. Bone Miner. Res.* **1995**, *10*, 453–457. [CrossRef] [PubMed]
61. Yamaguchi, M. Role of zinc in bone formation and bone resorption. *J. Trace Elem. Exp. Med.* **1998**, *11*, 119–135. [CrossRef]
62. Bowen, P.K.; Shearier, E.R.; Zhao, S.; Guillory, R.J.; Zhao, F.; Goldman, J.; Drelich, J.W. Biodegradable metals for cardiovascular stents: From clinical concerns to recent Zn-alloys. *Adv. Healthc. Mater.* **2016**, *5*, 1121–1140. [CrossRef] [PubMed]
63. Kaltenberg, J.; Plum, L.M.; Ober-Blobaum, J.L.; Honscheid, A.; Rink, L.; Haase, H. Zinc signals promote IL-2-dependent proliferation of T cells. *Eur. J. Immunol.* **2010**, *40*, 1496–1503. [CrossRef] [PubMed]
64. Shankar, A.H.; Prasad, A.S. Zinc and immune function: The biological basis of altered resistance to infection. *Am. J. Clin. Nutr.* **1998**, *68*, 447s–463s. [PubMed]
65. Kaur, G. Biodegradable metals as bioactive materials. In *Bioactive Glasses: Potential Biomaterials for Future Therapy*; Springer International Publishing: Cham, Switzerland, 2017.
66. Krezel, A.; Maret, W. The biological inorganic chemistry of zinc ions. *Arch. Biochem. Biophys.* **2016**, *611*, 3–19. [CrossRef] [PubMed]
67. Thomas, S.; Birbilis, N.; Venkatraman, M.S.; Cole, I.S. Corrosion of zinc as a function of pH. *J. Sci. Eng.* **2012**, *68*. [CrossRef]
68. Drelich, A.; Zhao, S.; Guillory, R.J.; Drelich, J.W.; Goldman, J. Long-term surveillance of zinc implant in murine artery: Surprisingly steady biocorrosion rate. *Acta Biomater.* **2017**, *58*, 539–549. [CrossRef] [PubMed]
69. Shearier, E.R.; Bowen, P.K.; He, W.; Drelich, A.; Drelich, J.; Goldman, J.; Zhao, F. In vitro cytotoxicity, adhesion, and proliferation of human vascular cells exposed to zinc. *ACS Biomater. Sci. Eng.* **2016**, *2*, 634–642. [CrossRef] [PubMed]
70. Zhu, D.H.; Su, Y.C.; Young, M.L.; Ma, J.; Zheng, Y.F.; Tang, L.P. Biological responses and mechanisms of human bone marrow mesenchymal stem cells to Zn and Mg biomaterials. *ACS Appl. Mater. Interfaces* **2017**, *9*, 27453–27461. [CrossRef] [PubMed]
71. Qiao, Y.Q.; Zhang, W.J.; Tian, P.; Meng, F.H.; Zhu, H.Q.; Jiang, X.Q.; Liu, X.Y.; Chu, P.K. Stimulation of bone growth following zinc incorporation into biomaterials. *Biomaterials* **2014**, *35*, 6882–6897. [CrossRef] [PubMed]
72. Al Qaysi, M.; Petrie, A.; Shah, R.; Knowles, J.C. Degradation of zinc containing phosphate-based glass as a material for orthopedic tissue engineering. *J. Mater. Sci.* **2016**. [CrossRef]

73. Zhong, Z.; Ma, J. Fabrication, characterization, and in vitro study of zinc substituted hydroxyapatite/silk fibroin composite coatings on titanium for biomedical applications. *J. Biomater. Appl.* **2017**, *32*, 399–409. [CrossRef] [PubMed]
74. Yu, J.M.; Xu, L.Z.; Li, K.; Xie, N.; Xi, Y.H.; Wang, Y.; Zheng, X.B.; Chen, X.S.; Wang, M.Y.; Ye, X.J. Zinc-modified calcium silicate coatings promote osteogenic differentiation through TGF-β/Smad pathway and osseointegration in osteopenic rabbits. *Sci. Rep.* **2017**, *7*, 3440. [CrossRef] [PubMed]
75. Cama, G.; Nkhwa, S.; Gharibi, B.; Lagazzo, A.; Cabella, R.; Carbone, C.; Dubruel, P.; Haugen, H.; Di Silvio, L.; Deb, S. The role of new zinc incorporated monetite cements on osteogenic differentiation of human mesenchymal stem cells. *Mater. Sci. Eng. C* **2017**, *78*, 485–494. [CrossRef] [PubMed]
76. Ferreira, E.C.S.; Bortolin, R.H.; Freire-Neto, F.P.; Souza, K.S.C.; Bezerra, J.F.; Ururahy, M.A.G.; Ramos, A.M.O.; Himelfarb, S.T.; Abreu, B.J.; Didone, T.V.N.; et al. Zinc supplementation reduces RANKL/OPG ratio and prevents bone architecture alterations in ovariectomized and type 1 diabetic rats. *Nutr. Res.* **2017**, *40*, 48–56. [CrossRef] [PubMed]
77. Yu, W.L.; Sun, T.W.; Qi, C.; Ding, Z.Y.; Zhao, H.K.; Zhao, S.C.; Shi, Z.M.; Zhu, Y.J.; Chen, D.Y.; He, Y.H. Evaluation of zinc-doped mesoporous hydroxyapatite microspheres for the construction of a novel biomimetic scaffold optimized for bone augmentation. *Int. J. Nanomed.* **2017**, *12*, 2293–2306. [CrossRef] [PubMed]
78. Yusa, K.; Yamamoto, O.; Takano, H.; Fukuda, M.; Iino, M. Zinc-modified titanium surface enhances osteoblast differentiation of dental pulp stem cells in vitro. *Sci. Rep.* **2016**, *6*. [CrossRef] [PubMed]
79. An, S.F.; Gong, Q.M.; Huang, Y.H. Promotive effect of zinc ions on the vitality, migration, and osteogenic differentiation of human dental pulp cells. *Biol. Trace Elem. Res.* **2017**, *175*, 112–121. [CrossRef] [PubMed]
80. Bowen, P.K.; Guillory, R.J.; Shearier, E.R.; Seitz, J.-M.; Drelich, J.; Bocks, M.; Zhao, F.; Goldman, J. Metallic zinc exhibits optimal biocompatibility for bioabsorbable endovascular stents. *Mater. Sci. Eng. C* **2015**, *56*, 467–472. [CrossRef] [PubMed]
81. Yang, H.; Wang, C.; Liu, C.; Chen, H.; Wu, Y.; Han, J.; Jia, Z.; Lin, W.; Zhang, D.; Li, W.; et al. Evolution of the degradation mechanism of pure zinc stent in the one-year study of rabbit abdominal aorta model. *Biomaterials* **2017**, *145*, 92–105. [CrossRef] [PubMed]
82. Lansdown, A.B. Silver in health care: Antimicrobial effects and safety in use. In *Biofunctional Textiles and the Skin*; Karger: Basel, Switzerland, 2006.
83. Mertz, W. *Trace Elements in Human and Animal Nutrition*; Academic Press, INC.: Orlando, FL, USA, 1986.